

VLT observations of the peculiar globular cluster NGC 6712, II: luminosity and mass functions*

G. Andreuzzi^{1,2}, G. De Marchi^{2,3,4}, F. R. Ferraro^{5,2}, F. Paresce², L. Pulone¹, and R. Buonanno¹

¹ Osservatorio Astronomico di Roma, via di Frascati 33, I-00040 Monteporzio Catone, Rome, Italy

² European Southern Observatory, Karl-Schwarzschild-Strasse 2, D-85748 Garching, Germany

³ Space Telescope Science Institute, 3700 San Martin Drive, Baltimore, MD 21218, USA

⁴ affiliated with the Astrophysics Division, Space Science Department, European Space Agency

⁵ Osservatorio Astronomico di Bologna, Via Ranzani 1, I-40127, Bologna, Italy

Received 16.9.2000; accepted 13.3.2001

Abstract. We have carried out extensive VLT–FORS1 observations covering a fair fraction of the intermediate metallicity globular cluster NGC 6712 in the V and R bands. We derive accurate colour–magnitude diagrammes (CMD) and luminosity functions (LFs) of the cluster main sequence (MS) for four overlapping fields extending from the centre of the cluster out to a radius of $\sim 10'$, well beyond the nominal tidal radius, and for a control field at $\sim 42'$ distance. The LFs extend from the cluster turn-off (TO) at $M_R \simeq 4$ to the point at which the incompleteness drops below 50% (corresponding to $R \simeq 23$ or $M_R \simeq 7.5$) for most fields studied. Cluster stars become indistinguishable from field stars at $r \simeq 5'$. The shape of the cluster’s LF and its variation with distance from the centre in these ranges are well described by a standard multi-mass static model having the following parameters: core radius $r_c = 1'$, half-light radius $r_{hl} = 1.8'$, tidal radius $r_t = 5.2'$, concentration ratio $c = 0.7$, and a power-law global mass function (MF) with index $\alpha \simeq 0.9$ for masses smaller than $0.8 M_\odot$, i.e. for all detected MS stars, and $\alpha \simeq -2.35$ for evolved objects. The MF obtained in this way is consistent with that found in a preliminary investigation of this cluster with the VLT Test Camera and confirms that this is the only globular cluster known so far for which the global MF drops with decreasing mass below the TO. Possible reasons for this unique characteristic are discussed with the most likely associated with its extreme vulnerability to tidal disruption.

Key words: globular clusters: general – globular clusters: individual: NGC 6712 – stars: luminosity function, mass function – stars: low-mass, brown dwarfs – stars: Population II

1. Introduction

NGC 6712 ($\alpha = 18^h 53^m 04.3''$, $\delta = -08^\circ 42' 21.5''$) is a small and sparse globular cluster of intermediate metallicity (concentration ratio $c = 0.9$ and $[\text{Fe}/\text{H}] = -1.01$; Harris 1997). Cudworth (1988), in his astrometric and photometric study reaching down to just above the main sequence TO, finds that it is a halo object in spite of its moderately high metallicity. One interesting characteristic of this cluster is the presence in the core of the high luminosity X-ray source (X1850-086) with an optical counterpart (Anderson et al. 1993). This is unexpected for such a loose cluster because most clusters with such sources tend to have a much higher central concentration. To explain this peculiarity, Grindlay et al. (1988) have suggested that the cluster may be currently re-expanding following the phase of core collapse when densities were high enough to allow these binaries to be formed. Our discovery (Ferraro et al., 2000) of the presence in the core of another close binary, a UV- and $H\alpha$ -excess object, most likely a quiescent LMXB or a CV, only adds to the mystery.

Another, possibly connected and potentially even more interesting facet of this cluster’s structure is the fact that the first observations of its MS taken by the VLT during its commissioning period and reported by De Marchi et al. (1999) show a remarkable property of its MF near the half-light radius. This is a clear and continuous drop with decreasing mass starting already at the TO and continuing down to the observation limit at $\simeq 0.5 M_\odot$. MFs determined from LFs obtained near the half-light radius are expected to faithfully reflect the shape of the cluster’s global MF (De Marchi et al. 2000; Vesperini & Heggie 1997). For all the other clusters surveyed so far with HST in this mass range, the global MF increases steadily with decreasing mass (Paresce & De Marchi 2000).

As suggested by De Marchi et al. (1999), this may be due to the fact that its Galactic orbit forces the cluster to penetrate deeply into the bulge. With a perigalactic distance smaller than 300 pc, this cluster ventures so

Send offprint requests to: G. De Marchi (demarchi@stsci.edu)

* Based on data obtained as part of an ESO Service Mode programme

frequently and so deeply into the Galactic bulge (Dauphole et al. 1996) that it is likely to have undergone severe tidal shocking during the numerous encounters with both the disk and the bulge during its life-time. The latest Galactic plane crossing could have happened as recently as 4×10^6 year ago (Cudworth 1988), which is much smaller than its half-mass relaxation time of 1 Gyr (Harris 1996). It is precisely on this basis that Takahashi & Portegies Zwart (2000) have suggested that NGC 6712 has lost 99 % of its mass during its life-time. And if the effects of this strong interaction have propagated throughout the whole cluster and reached its innermost regions, as such a gigantic mass loss implies, the peculiarly high density of core binaries can be understood and justified for what would otherwise appear an inconsequential cluster.

In an attempt to clarify this important issue and to better understand the observable effects of tidal interactions, and especially to learn more about the mechanisms leading to the dissolution of globular clusters in the Galaxy and about the possible variation of the cluster IMF with time in general, we have used the great power of the VLT and the FORS1 camera to investigate in more detail the present structure of NGC 6712. The specific objective was to obtain a more precise LF of the MS below the TO at various distances from the centre, so as to evaluate the possible effects of mass segregation on the derived MF. Another important objective was to sample more of the cluster at or near the tidal radius to see whether or not one could detect an excess of low mass stars ejected from the interior and still lightly bound to the cluster and to correct for the numerous field stars expected in the cluster field. In this paper, we report on the results of the analysis of our VLT data set on NGC 6712 with an emphasis on the cluster MS. The analysis of the evolved part of the cluster CMD is the subject of other papers (Ferraro et al. 2000; Paltrinieri et al. 2001).

2. Observations and data reduction

Our data consist of images of 5 fields in the *V* and *R* bands, four of which are located as shown in Fig. 1. The fifth field, used as a control field (field F0), is located $42' \text{ N}$ of the cluster centre and was imaged using FORS1 in its standard resolution mode of $0''.2/\text{pixel}$.

Because the level of crowding varies considerably from the core of the cluster out to its periphery, our observations were carried out according to the following strategy: the fields covering the external regions of the cluster were imaged at low resolution (plate-scale $0''.2/\text{pixel}$) and cover an area of 46.2 arcmin^2 each ($6'.8 \times 6'.8$); they are located respectively $5' \text{ W}$ (field F2), $8' \text{ NW}$ (field F3) and $11' \text{ W}$ (field F4) of the centre of the cluster; to improve the photometry in the central regions, where the level of crowding is particularly high, we have covered it with images taken in the high resolution mode of FORS1 (plate-scale $0''.1/\text{pixel}$), with a field $3'.4 \times 3'.4$ in size (field

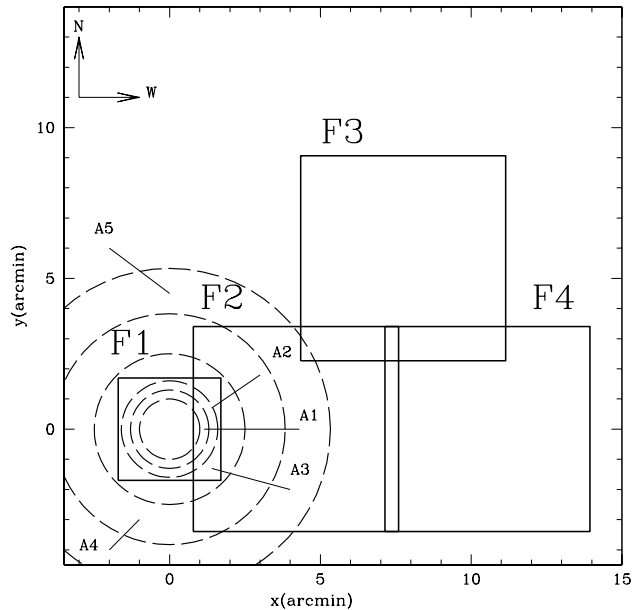


Fig. 1. Locations of the four FORS1 fields on NGC 6712. The centre of the cluster is located at the origin of the coordinate system. Dashed circles represent the annuli A1–A4 described in the text

F1, shown in Fig. 2). To ensure a homogeneous calibration and to transform the coordinates into a common local system from the centre of the cluster out to the more external regions, each field has been selected so as to overlap with at least a neighbouring one.

Since NGC 6712 is situated in the midst of a rich star field at the centre of the Scutum cloud (Sandage 1965), which is one of the highest surface-brightness regions with high space-density gradients of the Milky Way (Karaali 1978), we were anticipating that we would have had to deal with significant foreground contamination and, therefore, took the control field F0 in a region situated well away from the cluster but representing a typical field in that area.

The journal of the observations is reported in Table 1, where the columns represent respectively: the fields covered, the date of each observation, the distance of the fields from the centre of the cluster and their coordinates, and the exposure time for the single images and for each filter. Also listed in Table 1 is the number of stars detected simultaneously in both filters for each observed field (see below).

Except for a small subset of the *R*-band images, we have adopted the reduced and calibrated (i.e. bias-subtracted and flat-fielded) data as provided by the standard ESO-VLT pipeline. Some of the raw *R*-band data, however, had not been processed through the automated pipeline, and for them we had to run standard IRAF routines following the same recipe employed in the ESO-

Table 1. Journal of the observations

Field	Date	<i>r</i>	α (2000)	δ (2000)	$t_R(s)$	$t_V(s)$	N_{obj}
F1	16.06.99	0	$18^h 53' 04''$	$-08^\circ 42' 22''$	180×4	180×4	23057
F2	15.06.99	5'	$18^h 52' 45''$	$-08^\circ 42' 22''$	900×2	900×4	18777
	09.07.99				900×2		
F3	14.06.99	8'	$18^h 52' 33''$	$-08^\circ 36' 42'$	900×4	900×4	16049
F4	08.06.99	11'	$18^h 52' 22''$	$-08^\circ 42' 22''$	900×4	900×4	24092
F0	20.06.99	42'	$18^h 53' 04''$	$-08^\circ 00' 22''$	900×4	900×4	24117

VLT pipeline. Subsequent data reduction and analysis was done using standard IRAF photometry routines (*digiphot.daophot*).

Since our goal was to reliably detect the faintest object in these images, for each field and filter we first created a mean frame using all the applicable frames available and then ran the standard *digiphot.daofind* routine on the average images so obtained to locate the stars. Typical values of the PSF-FWHM are $0.^{\circ}3$ and $0.^{\circ}7$, respectively at high and low resolution. Although, in principle, we could have also averaged images in different filters, the presence of bad columns in the *R*-band frames (usually due to heavily saturated pixels and spikes of the bright stars) suggested that we not follow this approach. With a detection threshold set in the *V* and *R* band typically at $3 - 5\sigma$ above the local average background level, we obtained two independent coordinate lists for each field (one per filter), which we then fed to the PSF-fitting routine *allstar* to measure the instrumental magnitude of each object in each filter. We found that a Moffat function gave the best representation of the shape of the PSF, both at high and low resolution.

The positions of the identified objects in each mean *R*- and *V*-band image were matched to one another, so as to obtain a final catalogue containing only the positions and magnitudes of the stars common to both filters.

Objects lying in overlapping regions between two adjacent fields were used to determine the transformations between instrumental magnitudes and to translate *local* frame coordinates to a *common* coordinate system, with origin at the cluster centre. Typically, about one hundred stars in each overlapping region were used to derive such transformations. Only linear transformations were used to match star measurements, with all magnitudes being referred to those of the high resolution field (F1). For stars in the overlapping region, multiple magnitude measurements were averaged using appropriate weights (which take into account the photometric quality of each field). At the end of this procedure, a homogeneous set of instrumental magnitudes, colours and positions (referred to field F1) were obtained for a total of 106092 stars, in F1, F2, F3 and F4.

Instrumental (F1) magnitudes were finally transformed to the standard Johnson system, using the stars in common with the bright portion of the CMD which

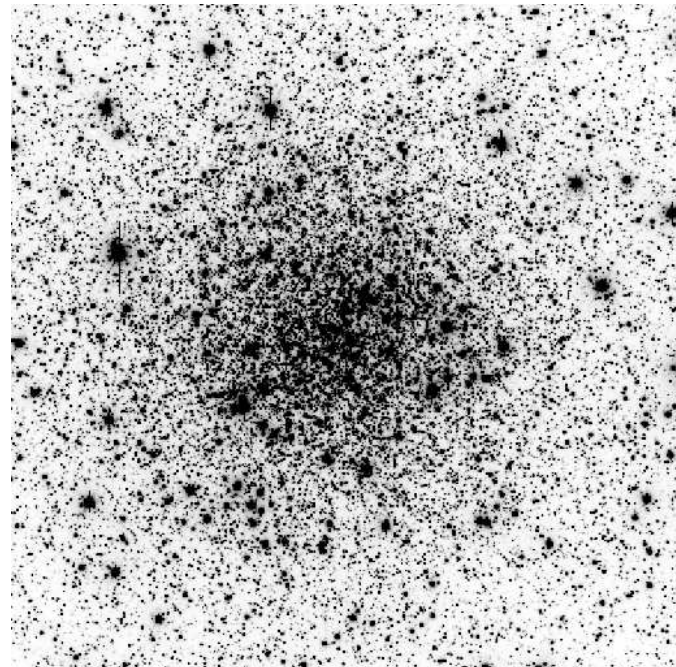


Fig. 2. VLT-FORS1 high resolution image (180s exposure) of the core of NGC 6712 in the *R* band (field F1). The size of the image is $3.^{\circ}4 \times 3.^{\circ}4$. North is up and East to the left

has been properly calibrated using 10 standard stars (see Paltrinieri et al. 2001).

Fig. 3 shows the total CMD of the central region of NGC 6712 (field F1). The figure is obtained by merging the deep (180s long exposure) and the bright (10s exposure) data covering the core of the cluster. In the following, we deal exclusively with the properties of the cluster MS (from the TO at $R \simeq 19$ to $R \simeq 23$; see Table 1) while the bright portion of the CMD and the properties of the evolved stellar population are discussed elsewhere (Ferraro et al. 2000; Paltrinieri et al. 2001).

2.1. Incompleteness corrections

A reliable assessment of the correction for incompleteness is a crucial step because the main goal of this work is to compare with one another the *R*-band LFs obtained at

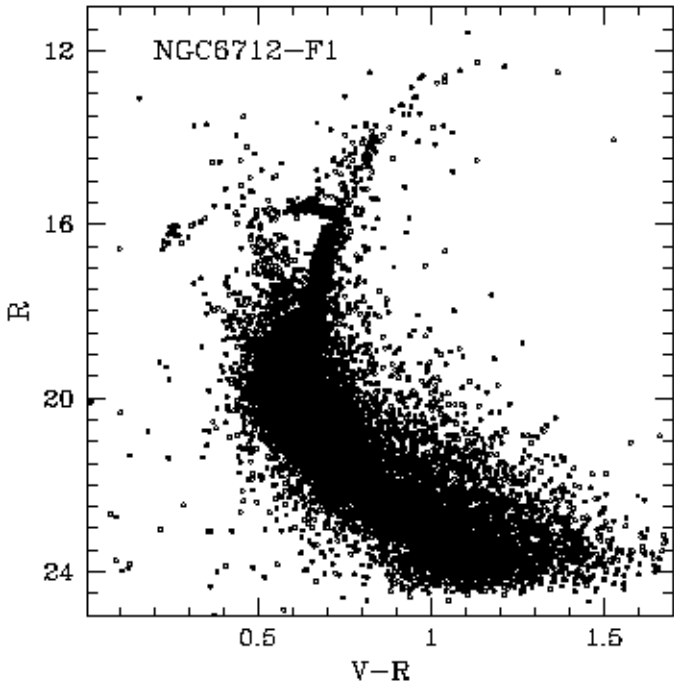


Fig. 3. Color-magnitude diagramme of the stars in field F1 (core) of NGC 6712

different radial distances from the centre of the cluster and to extract in this way information on the underlying global MF. Clearly, the completeness depends on the level of crowding in the observed fields and, therefore, on their location with respect to the cluster centre. In particular, an insufficient or inappropriate correction for crowding will result in the distortion of the stellar LF with a preferential loss of fainter stars and a relative increase of bright and spurious objects. In our case, crowding is not the only source of incompleteness: the distribution in luminosity of the stars is also modified by the large number of hot pixels and bad columns affecting the original images.

To correct our photometry for incompleteness, we ran artificial star tests on both sets of frames (V and R) independently, so as to be able to estimate the overall completeness of our final CMD. First, we applied the artificial star test to the mean R -band images: artificial stars in each given 0.5 magnitude bin were added randomly to the frames, making sure not to exceed a few percent ($\leq 10\%$) of the total number of stars actually present in that bin so as to avoid a significant enhancement of image crowding. We then added an equal number of stars at the same positions in the V -band frames and with a magnitude such that they would fall on the cluster MS. It should be noted that we made the assumption that all artificial stars were to lie on the MS since our intent was to verify the photometric completeness of MS stars. This procedure was repeated for all the bins of each field's CMD in both filters. To obtain a robust result, we simulated more than 200,000 stars in 250 artificial images for each field.

All pairs of V and R frames obtained in this way were then subjected to the same analysis used for the original frames, with the result being a catalogue of matching objects, each characterised by a position and a pair of V and R -band magnitudes. Each of these 250 catalogues (one per artificial pair of images) was compared with the catalogue of input artificial stars: an artificial star was considered detected only when its final position and magnitudes were found to coincide with the input catalogue to within Δx , $\Delta y \leq 1.5$ pixel, $\Delta \text{mag} \leq 0.3$. This approach allowed us to build a map showing how photometric completeness varies with position in our frames.

If N_{rec} is the number of recovered stars in a given magnitude bin, and N_{sim} the number of the simulated stars in the same bin, the ratio $N_{\text{rec}}/N_{\text{sim}} = \Phi$ gives the completeness in that bin for the location considered.

2.2. Field subtraction

In addition to correcting for photometric incompleteness, a reliable determination of the LF of NGC 6712 requires that we account for the contamination caused by field stars. We have dealt with this correction in a statistical way by using the comparison field F0, for which we have produced a CMD and assessed photometric incompleteness precisely as we did for all other fields. When it comes to measuring the LF – our final goal – we subtract from the stars found in a given magnitude bin on the cluster CMD the objects detected in the same magnitude bin in an area of equal size on the F0 field. Clearly, both numbers are corrected for their respective photometric incompleteness before doing the subtraction.

By applying the statistical field star subtraction described above, we discovered that stars located in fields F3 and F4 can be considered as belonging to the field because all the objects in the CMD of these fields are statistically compatible with being field stars. We show this in Fig. 4, where we plot the R -band LF, corrected for incompleteness, as measured in fields F3 and F0 (the solid and dashed lines, respectively). The absence of any significant trend or systematic departures of one function with respect to the other (to within 2σ) confirms that there are no residual cluster stars at distances greater than $\sim 5'$ from the cluster centre. As a result of this finding, we decided to consider all stars lying in F3 and F4 as field stars, thus improving the statistical sample of the field, and re-defined the decontamination procedure above using as a comparison field the whole catalogue for F3, F4 and F0 ($r \geq 5'$). This result also shows that the field around NGC 6712 is relatively uniform at our required level of accuracy and further confirms that the statistical decontamination correction that we apply is reliable.

We, therefore, regarded only the F1 and F2 fields as containing cluster stars. Because of the richness of our sample of stars, we decided to investigate the variation of the LF as a function of distance on a scale smaller than

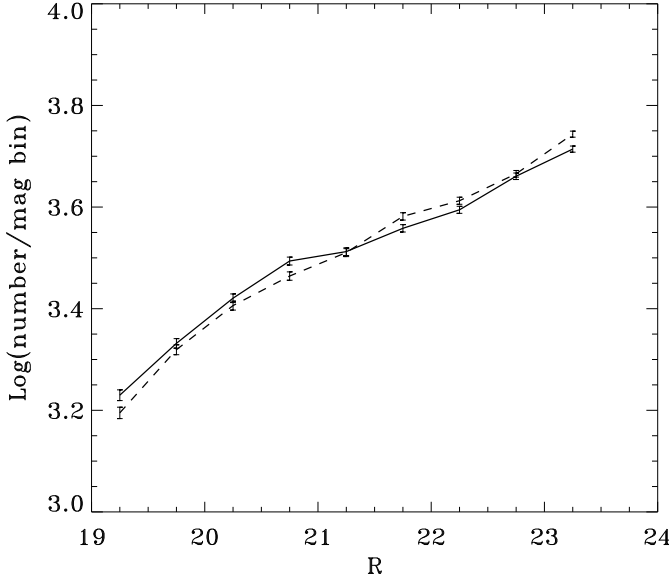


Fig. 4. Luminosity functions measured in fields F0 (dashed line) and F3 (solid line)

the typical size of a frame. We have, thus, divided our combined photometric catalogue into a number of annuli which are centered on the cluster centre and whose size increases with distance so as to guarantee a similar number of objects in each of them. Table 2 lists the five annuli A1 – A5 that we have used, whose positions are also marked in Fig. 1. The columns in Table 2 represent, respectively, the position and size of these annuli and the number of objects measured before (N) and after (N_S) the statistical decontamination. N is the number of objects in the range $19 < R < 22$ in each annulus before subtraction for field stars, while N_S is the number of objects after that subtraction in the same range (selected so as to have photometric completeness always $> 50\%$ in each annulus). Correction for photometric incompleteness is always applied before performing the subtraction. We note here that annulus A3 is not properly annular in shape, in that it extends from a radius of $96''$ all the way to the edge of field F1. The outer radius given in Table 2 ($105''$) is that which an annulus of equivalent area would have.

Table 2. Location of the annuli A1 – A5 in arcsec and in units of r_h (1'3; Djorgovski 1993); see text for the definition of N and N_S

Annulus	$r/1''$	r/r_h	N	N_S
A1	60 - 78	0.77 - 1.00	4335	3573
A2	78 - 96	1.00 - 1.23	3742	2794
A3	96 - 116	1.23 - 1.34	3433	2169
A4	150 - 230	1.92 - 2.94	4434	744
A5	230 - 320	2.94 - 4.1	4053	72

We did not use the innermost regions of the cluster ($r \leq 60''$), as the high level of crowding and the large

ensuing incompleteness would have resulted in a poor determination of the LF. Moreover, we did not include a region between annuli A3 and A4 because the level of crowding there is too high for the low resolution of the FORS1 camera at $0''.2/\text{pixel}$ and a standard seeing quality of $\text{FWHM} \simeq 0''.6$.

3. The luminosity function

We have determined the R -band LF in each one of the annuli A1 – A5 by counting the number of stars in bins of 0.5 magnitude each as a function of the R magnitude and correcting these values for photometric incompleteness (see Sect. 2 above). The same procedure was applied to the comparison fields, and the number of stars found in this way was subtracted from the LF of annuli A1 – A5, after having properly rescaled it so as to account for the different area covered by the annuli and by the comparison field.

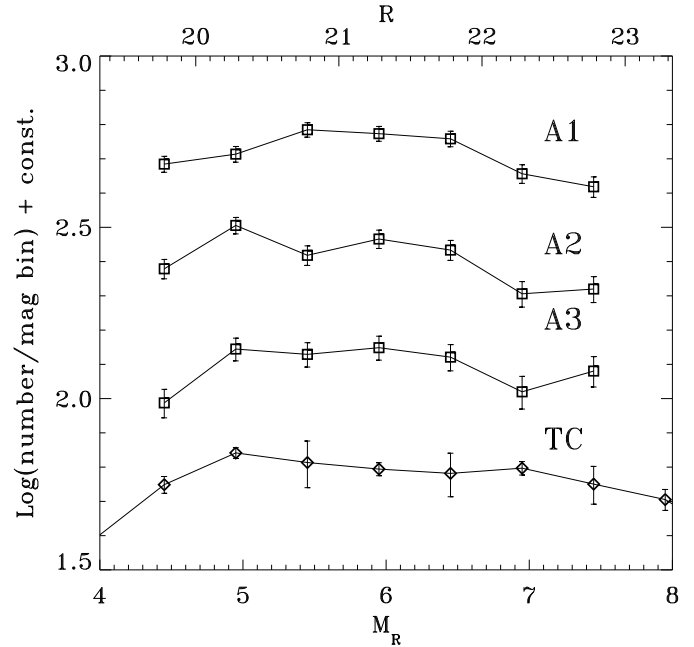


Fig. 5. The LFs measured in annuli A1 – A3, after correction for photometric incompleteness and for field star contamination, are here compared with the LF derived by De Marchi et al. (1999) with the VLT-TC further out in the cluster (see text)

Analysis of the LF of annuli A4 and A5 suggests that, in the region covered by these annuli, the cluster population starts to become negligible with respect to the field (see Table 2), and the completeness drops severely below 50% at $R > 22$. In particular, the LF of annulus A5 oscillates statistically around zero. In the following we, therefore, focus our investigation only on the region covered by the first three annuli. The LF obtained in this way in annuli A1 – A3 are listed in Table 3 and shown graphically

in Fig. 5 (boxes). Error bars in Fig. 5 reflect the total error associated with each bin and include both the Poisson statistical error and the uncertainty due to the correction for incompleteness:

$$\sigma_{bin} = \frac{\sqrt{N}}{\Phi} + \frac{N\sigma_{\Phi}}{\Phi^2} \quad (1)$$

where N is the number of stars before correction for incompleteness, Φ and σ_{Φ} are the completeness factor and the associated errors (ranging from $\sigma_{\Phi} \simeq 0.01$ to $\simeq 0.03$). We note here that the equation above provides a conservative (upper limit) estimate of the uncertainty and is based on the formalism developed by Bolte (1989). To account for the errors introduced by the statistical subtraction of the comparison field, we have combined in quadrature the σ_{bin} of each annulus with that of the comparison field. It should also be noted here that, the very good agreement between the field LFs shown in Fig. 4 and measured $\sim 40'$ away from one another suggests that our LFs are not likely to be affected by local fluctuations in the distribution of contaminating field stars.

Inspection of Fig. 5 immediately reveals that the three LFs, measured at different radial distances from the centre of the cluster in the range $60''$ to $105''$ ($0.77 r_h$ to $1.34 r_h$), are rather similar to one another: except for a modest increase with decreasing luminosity up to $R \simeq 20.5$, they are substantially flat or slightly decreasing down to $R \simeq 23$, where the completeness drops below $\sim 50\%$.

An interesting check is to compare the LF in our annuli with that derived by De Marchi et al. (1999) in a region of the cluster at a slightly larger radial distance ($r = 135''$) and located within our zone of avoidance (see Sect. 2) between annuli A3 and A4. This comparison is shown in Fig. 5, in units of absolute R -band magnitude. To convert our measurements from R to M_R we have adopted a distance modulus in the R band of $(m - M)_R = 15.33$ (see Paltrinieri et al. 2001), which differs only marginally from the value of $(m - M)_R = 15.31$ used by De Marchi et al. (1999). An inspection of this figure confirms that for NGC 6712 the LFs obtained at different radial distances from the centre have a similar shape and, over the magnitude range common to all of them, they are consistent with one another within the quoted errors in the region from $60''$ to $135''$.

This result is reassuring in that it confirms the validity of the inverted MF found by De Marchi et al. (1999; see Sect. 5 below). One should note here that De Marchi et al. could not use a comparison field to correct their LF for field star contamination and, because of this, they suggest that the number of stars in their LF was likely to be overestimated at the faint end, since the field LF is expected to increase steadily with magnitude. As it turns out, however, field stars account for a small fraction of the total stellar population in these regions, with cluster stars being from ~ 4 to ~ 2 times more numerous at $R \simeq 21.5$ (respectively in annuli A1 and A3). This fact, coupled with

the slow rate of increase of the field LF with magnitude (see Fig. 4), makes field star contamination in the TC field not sufficient to significantly alter the shape of the LF.

4. The global mass function

In Fig. 6, we compare the local MF obtained in annuli A1 – A3 using FORS1 with that measured by De Marchi et al. (1999) with the TC at $r = 135''$. Rather than converting the three individual LFs of annuli A1–A3 into MFs, we have first combined them into one single function by averaging their values in each magnitude bin, and have taken the standard deviation as a measure of the associated uncertainty (error bars). We have done that for compatibility with the approach used by De Marchi et al. (1999) for the LF obtained with the TC, and because the LFs of the three annuli are very similar to one another. In all cases (FORS1 and TC), we have obtained the MF by dividing the corresponding average LF by the derivative of the mass–luminosity (ML) relation appropriate for the metallicity of NGC 6712 ([Fe/H] = -1.01 ; Harris 1997). We plot here the results obtained using the ML relation of

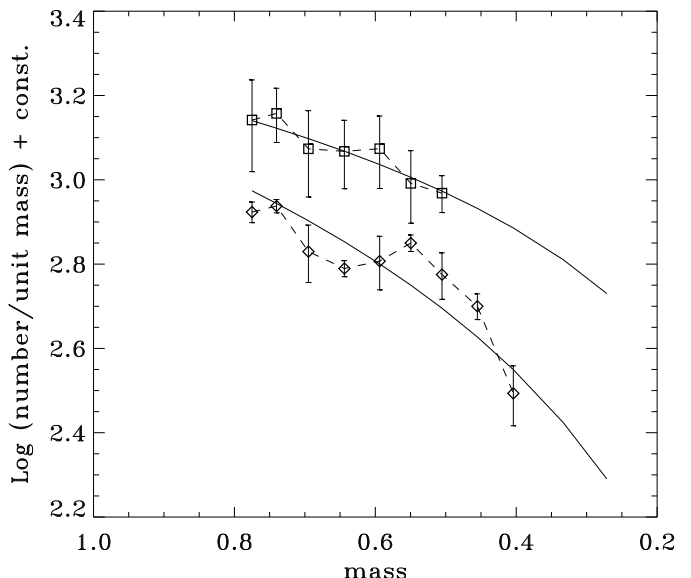


Fig. 6. Comparison between the average MF in annuli A1 – A3 (boxes) and that derived by (De Marchi et al. 1999) with the VLT-TC (diamonds) farther out in the cluster (see text). Thick solid lines mark the best fitting power-law, with index respectively $\alpha = 0.9$ and $\alpha = 1.5$

Baraffe et al. (1997), but using the models of Cassisi et al. (2000) would have yielded an almost identical result. The MFs derived in this way are shown in Fig. 6, where boxes connected by dashed lines represent the average of the MF in annuli A1 – A3 (upper curve) and in the TC field (lower curve), whereas the thick solid lines show the best fitting power-law MF, with index $\alpha = 0.9$ and $\alpha = 1.5$, respectively for the FORS1 data (upper curve) and TC

Table 3. Luminosity functions for annuli A1, A2, A3, and for the stars belonging to the control field in the R band. In particular, mag-bin is the centre of the bin used to obtain the LF; N is the actual number of stars observed; Φ is the completeness factor in each bin; N_C is the number of stars after the correction for incompleteness; N_S is the number of stars after the subtraction for the control field, properly rescaled; and σ is the standard deviation of the associated uncertainty

mag-bin		A1					A2					A3				
R	M_R	N	Φ	N_C	N_S	σ	N	Φ	N_C	N_S	σ	N	Φ	N_C	N_S	σ
19.75	4.42	530	0.91	582	484	25	462	0.92	502	379	24	359	0.88	407	244	23
20.25	4.92	536	0.84	638	517	27	566	0.86	658	507	28	485	0.88	551	350	26
20.75	5.42	585	0.78	750	609	29	496	0.84	590	415	27	486	0.85	571	338	27
21.25	5.92	514	0.69	744	593	29	515	0.79	651	463	28	478	0.79	605	354	28
21.75	6.42	433	0.58	746	573	29	465	0.72	645	430	28	477	0.77	619	332	29
22.25	6.92	333	0.52	640	453	28	382	0.69	553	321	27	413	0.72	573	263	28
22.75	7.42	315	0.50	630	415	28	359	0.60	598	331	28	415	0.63	658	302	30

data (lower curve). We should note here, however, that ignoring the data-point at $\sim 0.4 M_\odot$ in the lower curve would result in two MFs that agree perfectly well with one another, within the errors, and the best fitting power-law to the TC data would also have $\alpha \simeq 0.9$ (this agreement is hardly surprising as it was already implied by the remarkable similarity of the LF). Regardless of the last data-point, however, the net result in both cases is that *the number of stars decreases steadily with mass*.

This result gives strong support to the claim of De Marchi et al. that there is a relative deficiency of low mass stars with respect to the stars at the TO ($M \simeq 0.75 M_\odot$), although our data do not reach deep enough to see whether this observed drop continues all the way to $\sim 0.3 M_\odot$ where all known GC feature a peak in their MF (Paresce & De Marchi 2000) before plunging to the H-burning limit.

The dynamical evolution of a cluster depends on both the interaction among the stars in the cluster, which locally modifies the distribution of masses (internal dynamics, i.e. mass segregation), and on the interaction with the Galaxy. In our particular case, even though NGC 6712 is likely to have experienced strong tidal shocks during its life-time (De Marchi et al. 1999; Takahashi & Portegies Zwart 2000), one wonders whether the almost identical LFs (and ensuing MFs) that we observe at the various radial distances as shown in Fig. 5 can be ascribed to the internal two-body relaxation mechanism.

To address this issue more specifically, we have simulated the dynamical structure of the cluster using a multi-mass Michie–King model constructed with an approach close to that of Gunn & Griffin (1979), as extensively described in Meylan (1987; 1988), and following the technique developed more recently by Pulone et al. (1999) and De Marchi et al. (2000), to whom we refer the reader for further details.

Each model is characterized by three structural parameters describing, respectively, the scale radius (r_c), the scale velocity (v_s), the central value of the gravitational potential (W_o), and a global MF of the form $dN \propto m^\alpha$,

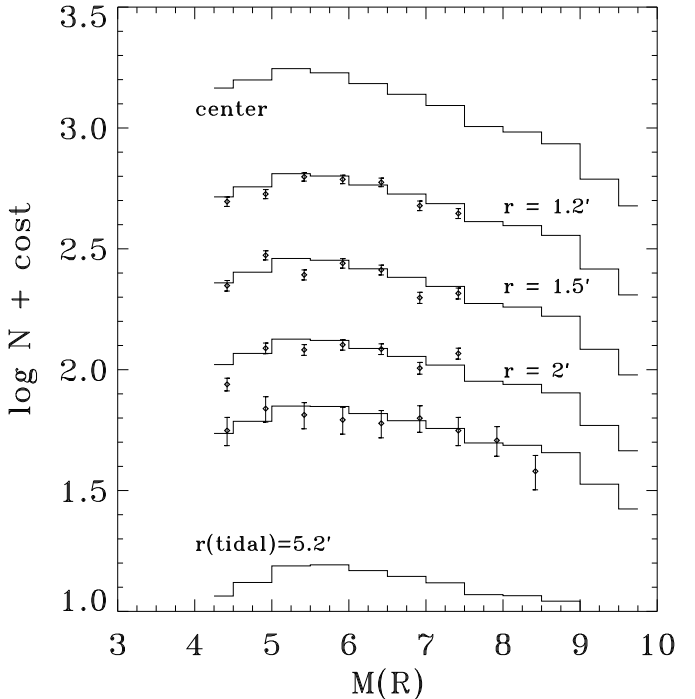


Fig. 7. Theoretical LF as a function of distance as predicted by the multi-mass Michie–King model described in the text. Diamonds represent the observed LFs in annuli A1 – A3, and in the TC field

where the exponent α would equal -2.35 in the case of Salpeter's IMF. Stellar masses have been distributed into nineteen different mass classes, covering MS stars, white dwarfs (WDs) and other heavy remnants. All stars lighter than $0.8 M_\odot$ have been considered still on their MS, while heavier stars with initial masses in the range $8.5 – 100 M_\odot$ have been assigned a final mass of $1.4 M_\odot$. WD have been subdivided into three mass classes, following the prescriptions of Meylan (1987; 1988) and assigned to the corresponding MS mass using the relations presented by Weidemann (1988) and Bragaglia et al. (1995). The lower mass limit is assumed to be $0.085 M_\odot$. As already shown by

Meylan (1987), the exact value of different mass cutoffs does not significantly influence the result of the dynamical modelling.

In order to fit the structural parameters of NGC 6712, two different mass function exponents have been adopted: α_{up} for stellar masses in the range $0.8 - 100 M_{\odot}$, and α_{ms} for MS stars below $0.8 M_{\odot}$. We have furthermore assumed complete isotropy in the velocity distribution.

From the parameter space, we have considered only those models characterised by a surface brightness profile (SBP), a velocity dispersion profile (VDP) and a mass-to-light (M/L) ratio which would simultaneously agree well with their corresponding observed values. We have further constrained the choice among the best fitting dynamical models with the smallest reduced chi-squares, by imposing the condition that the four observed LFs (A1–A3 and TC) had to be simultaneously fitted by their theoretical counterparts as predicted by the mass stratification of the dynamical structure of the cluster (see Pulone et al. 1999 and De Marchi et al. 2000 for an extensive description of this technique). As regards the SBP of NGC 6712, in our simulations we have followed the approach of Trager et al. (1985) and have used its Chebyshev polynomial fit as evaluated on our own data (see Fig. 8), while for the VDP we have used the mean values obtained by Grindlay et al. (1988) within about three core radii. The value of $M/L = 0.7$ has also been taken from Grindlay et al. (1988).

Thanks to the many observational constraints that we force our model to satisfy, we are able to considerably reduce the space in which parameters can range. The best fitting set of parameters requires the indexes of a power-law global MF α_{up} and α_{ms} to take on values respectively around -2.3 (the Salpeter slope) and 0.9 , as shown in Fig. 7. The line of sight velocity dispersion at the centre is in this case $\sigma_v = 4.3 \text{ km s}^{-1}$ and the derived mass–luminosity ratio turns out to be $M/L = 0.74$, in perfect agreement with Grindlay et al.’s (1988) values $\sigma_v = 4 \text{ km s}^{-1}$ and $M/L = 0.7$. The key result here, then, is that the global MF of NGC 6712 is indeed an inverted function, i.e. one that decreases with decreasing mass below $\sim 0.8 M_{\odot}$. The other parameter values of the best fitting model are: core radius $r_c = 1'$, half-light radius $r_{\text{hl}} = 1.8'$, tidal radius $r_t = 5.2'$, concentration ratio $c = 0.7$, total mass of the cluster $M_{\text{cl}} = 7 \times 10^4 M_{\odot}$, mass fraction in heavy remnants $f = 0.6$.

A large fraction of mass in the form of white dwarfs, neutron stars and black holes such as the one that we find here might be surprising. Heavy remnants are usually thought to account for up to $20 - 30\%$ of the mass of a cluster (Meylan & Heggie 1997), whereas our result suggests at least twice as many. The amount of heavy remnants depends here exclusively on the shape of the IMF for stars more massive than $0.8 M_{\odot}$. Because the latter have already evolved off the MS and are no longer observable, the value of α_{up} is not as strongly constrained in our model

as is that of α_{ms} for less massive stars. If, for instance, a value of $\alpha_{\text{up}} = -6$ were used, the fraction of heavy remnants could be brought down to $\sim 25\%$. Besides being highly suspicious in a mass range where all known stellar populations display a Salpeter-like IMF (see e.g. Kroupa 2001), such a steep MF exponent would also strongly affect the M/L ratio, forcing it to take on the value of ~ 0.2 , which is very discordant with the $M/L = 0.7$ measured by Grindlay et al. (1988). We, therefore, leave the value of α_{up} unchanged and consider in the next section the observational consequences that the ensuing large fraction of heavy remnants implies.

The key result here, nevertheless, is that the current global MF of NGC 6712 is indeed an inverted function, i.e. one that decreases with decreasing mass, starting at least from $0.8 M_{\odot}$. Although all clusters whose LF has been studied in the core show an inverted local MF there (as a result of mass segregation: see e.g. Paresce et al. 1995; King et al. 1995; De Marchi & Paresce 1996), NGC 6712 is *the only known cluster so far* to feature an inverted MF on a global scale. McClure et al. (1985) and Smith et al. (1986) have observed a LF that drops with decreasing luminosity in the halo clusters E 3 (see also Veronesi et al. 1996) and Palomar 5, respectively. The actual shape of the corresponding global MF, however, is not known, as only a single field is available in each cluster. These objects are, nonetheless, very interesting and should be studied using deeper, higher resolution photometry at several locations in the clusters to properly address the effects of mass segregation.

5. Discussion and conclusions

As Fig. 7 confirms, the observed (small) variation of the shape of the LF with distance from the cluster centre is fully consistent with the mechanism of mass segregation ensuing from energy equipartition as currently understood in many other clusters (Meylan & Heggie 1997). We, therefore, cannot hold internal dynamical evolution responsible for the observed inverted global MF in NGC 6712: such a mechanism, in fact, could only account for the inverted MF near the core of the cluster, but not elsewhere (see De Marchi et al. 2000).

There remain, thus, only two ways to explain the inverted global MF of this cluster, as already proposed by De Marchi et al. (1999). Namely, either NGC 6712 was born with an inverted IMF, at least for stars less massive than $\sim 0.8 M_{\odot}$, or the interaction with the tidal field of the Galaxy (and more specifically disk and bulge shocking through its frequent and repeated perigalacticon passages) has imparted a strong modification to the stellar population of this cluster during its life-time, as its orbit forces it to penetrate deeply into the bulge at its disk crossings.

Although the former hypothesis cannot be completely ruled out, it is highly unsatisfactory as it would explain one anomaly — the inverted global MF — by invoking an-

other one, namely an inverted IMF. A careful investigation of the deep LF of a dozen GCs by Paresce & De Marchi (2000) shows no evidence of such an inverted IMF. Their sample does, admittedly, only cover $\sim 10\%$ of the total population of GC, but it contains clusters in widely different orbits and dynamical states so that it can be regarded as representative of the whole Galactic GC system. Still, the hypothesis of an inverted IMF cannot be excluded, at least until the origin of the inverted LF observed long ago in E 3 (McClure et al. 1985) and Pal 5 (Smith et al. 1986) is understood (see Sect. 4 above).

On the other hand, there seems to be more solid observational and theoretical support for the latter hypothesis, namely that the cluster has suffered severe tidal stripping which has remarkably altered its stellar population. Recent calculations of the orbit of NGC 6712 and consequent destruction rate by Gnedin & Ostriker (1997) and Dinescu et al. (1999) clearly suggest that it has one of the highest destruction rates of a large sample of Galactic GC and that it is one of the few objects for which the tidal-shock rate is higher than its two-body relaxation rate. One would, thus, expect that the strong tidal interaction during the disk crossings and the consequent tidal shocking should provoke a continuous loss of low-mass stars, especially from beyond the half-light radius, and a consequent rapid change of the stellar mass distribution. Precisely on this basis, Takahashi & Portegies Zwart (2000) have suggested that NGC 6712 has lost 99 % of its mass during its life-time and that it is now obviously only a pale remnant of its initial much more massive condition.

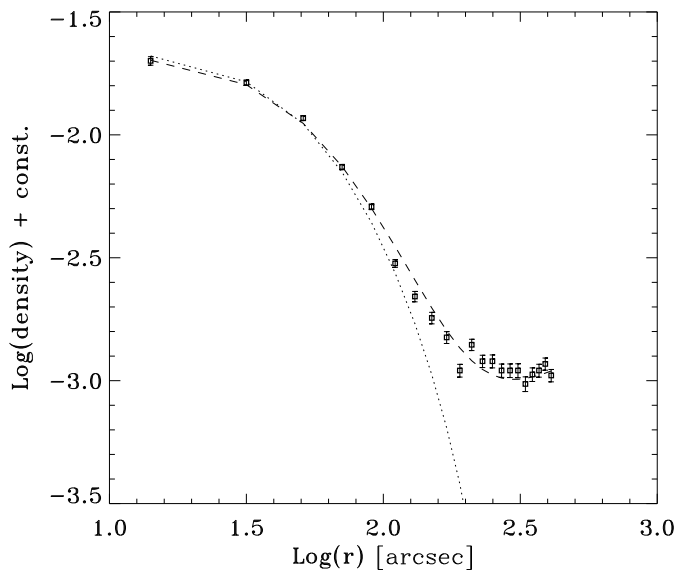


Fig. 8. Surface density profile of $\sim 0.75 M_{\odot}$ stars. The thin line shows a King-type profile with $r_c = 1'$ and $r_t = 5.2'$, whereas the thick dashed line shows the superposition of the latter on a plateau of field stars of uniform surface density.

One might wonder, however, how the internal dynamics of a cluster which has suffered such a tremendous mass loss could still conform so well to the predictions of standard two-body relaxation and energy equipartition as Fig. 7 indicates. Johnston et al. (1999), on the other hand, have shown that the tidal stripping operated by the Galaxy on a GC results in a steady differential loss of stars (light stars being dislodged more easily than massive ones) with the consequent continuous decrease of the exponent α of the global MF and the ensuing flattening of the latter. Although the inclination of the cluster's orbit determines the rate at which the MF exponent decreases, all orbits with perigalacticon within a few kpc of the Galactic centre are exposed to this erosion. For clusters such as NGC 6712, whose orbit is mostly contained within the disk (Dauphole et al. 1996), the heating due to disk and bulge shocking is diluted over a long time, comparable with the dynamical relaxation time of the cluster itself.¹ It is, thus, not unreasonable that two-body relaxation can proceed almost undisturbed, and it does so on a continuously varying mass spectrum.

A natural consequence of tidal stripping is the formation of tidal tails surrounding the cluster (Grillmair et al. 1995). While the latter might be relatively easy to identify around clusters on highly inclined orbits and currently well away from the Galactic plane, looking for extra-tidal populations around NGC 6712 is very difficult, because of its orbit and current location in the Galaxy, and even more so because the surface brightness of this excess of stars which might have been ejected from the interior but are still loosely bound to it is expected to be about 4 orders of magnitude lower than in the core (Johnston et al. 1999). We have, nevertheless, searched the region near the cluster's tidal radius ($> 5'$) but, not surprisingly, the radial density profile that we have measured does not reveal any obvious over-density near the cluster's boundary (see Fig. 8). On the other hand, we were forced to limit our investigation to stars in the range $19.5 < R < 20.5$ (i.e. to $\sim 0.75 M_{\odot}$ stars), so as to minimise the effects of variable photometric completeness and crowding with distance, and it is quite likely that most of these stars should today dwell preferentially in the central regions of the cluster, rather than in its periphery, as a result of mass segregation.

The radial density profile that we show in Fig. 8, however, has allowed us to define a more reliable tidal radius for this cluster. The thick dashed line marks a typical King-type profile with $r_c = 1'$ and $r_t = 5.2'$, superimposed on a plateau of field stars. A tidal radius of $\sim 5'$ is fully consistent with our finding of a statistically null cluster LF

¹ We note here that the half-mass relaxation time of $t_{hm} \simeq 1$ Gyr quoted by Harris (1996) is most likely an over-estimate for NGC 6712. A value of 1 Gyr is approximately the average t_{hm} for all GCs, and NGC 6712 is far less populous and smaller than the average Galactic cluster.

in annulus A5 (which extends to $r = 5.1'$). Although we have limited our analysis to stars for which photometric completeness is always $> 85\%$, severe crowding and the concentration of many saturated stars in the innermost regions could make our determination of the core radius r_c uncertain. Using shorter FORS1 exposures of the central $\sim 2'$ radius of this cluster, however, Paltrinieri et al. (2001) also find a value of $r_c \simeq 1'$, in excellent agreement with that estimated here.

Thus, assessing whether NGC 6712 was indeed much more massive in the past than it is now, as suggested by the work of Takahashi & Portegies Zwart (2000), would require a more accurate search for tidal tails surrounding the cluster, using a large field of view and sophisticated reduction techniques such as those developed by Grillmair et al. (1995) and, more recently, by Leon et al. (2000). On the other hand, the severe field contamination would necessarily limit the effectiveness of this technique. Moreover, even revealing the presence of tidal tails would not provide strong constraints on the original cluster mass. To be sure, tidal stripping has taken place throughout the whole life of the cluster and the majority of the stars lost in this way should be today totally unbound and dispersed elsewhere in the Galaxy.

A more precise, quantitative estimate of the original cluster mass could, however, come from a census of the WD population in its core. If NGC 6712 was indeed originally as massive as $10^7 M_\odot$, then a large number of WDs should now populate its core. Even ignoring the effects of mass segregation (which would further increase the WD population in the core by draining them from the periphery and forcing them to drift there by virtue of their higher mass), the prescriptions of Renzini (1985) suggest that ~ 2000 WDs brighter than $M_V \simeq 14$ ($V \simeq 28.5$) should dwell in the central $100''$ radius of the cluster, if the latter had its present mass ~ 5 Gyr ago. Clearly, if its mass that long ago was even only ten times as much as it is now, we would expect of order 20 000 WDs within a $100''$ radius. Already on the basis of the available data we can conclude that a large fraction ($\simeq 60\%$ or more) of the cluster's mass must be in the form of heavy remnants (see Sect. 4). Whether the cluster was originally only a few times more massive than it is now or whether it was one of the most massive in the Galaxy cannot be determined with certainty at present, although the N-body simulations of Vesperini & Heggie (1996) seem to suggest the latter option. With a powerful instrument such as the Advanced Camera for Surveys soon to be installed on board the HST, however, this scenario can easily be tested observationally and the suspected ongoing dissolution of NGC 6712 reliably characterised.

Acknowledgements. We are indebted to Carlton Pryor (the referee) whose comments and remarks have considerably strengthened the presentation of our results. It is our pleasure to thank Isabelle Baraffe for providing us with the tabulated theoretical M-L relations, and Barbara Paltrinieri for carrying

out the reduction of the short exposures of NGC 6712. G.A. gratefully acknowledges the hospitality of ESO through the Director General's Discretionary Research Fund. F.R.F. gratefully acknowledges the hospitality of the Visitor Programme during his stay at ESO when he contributed to this paper. G.A., R.B., F.R.F. and L.P. acknowledge the financial support of the Ministero della Università e Ricerca Scientifica e Tecnologica through the programme "Stellar Dynamics and Stellar evolution in Globular Clusters."

References

Anderson, S., Margon, B., Deutsch, E., Downes, R. 1993, AJ 106, 1049
 Baraffe, I., Chabrier, G., Allard, F., Hauschildt, P. 1997, A&A, 327, 1054
 Bolte, M. 1989, ApJ, 341, 168
 Bragaglia, A., Renzini, A., Bergeron, P. 1995, ApJ, 443, 735
 Cassisi, S., Castellani, V., Ciarcelluti, P., Piotto, G., Zoccali, M. 2000, MNRAS, 315, 679
 Cudworth, K. M., 1988A, AJ 96, 105
 Dauphole, B., Geffret, M., Colin, J., et al. 1996, A&A, 313, 119
 De Marchi, G., Leimbundgut, B., Paresce, F., Pulone, L. 1999, AA 343, L9
 De Marchi, G., Paresce, F. 1996, ApJ, 467, 658
 De Marchi, G., Paresce, F., Pulone, L., 2000, ApJ 530, 342
 Dinescu, D., Girard, T., Van Altena, W. 1999, AJ, 117, 1792
 Djorgovski, S., 1993, in ASP Conf. Ser. 50, eds. S. Djorgovski & G. Meylan (San Francisco: ASP), 373
 Ferraro, F., Paltrinieri, B., Paresce, F., De Marchi, G. 2000, ApJ, 542, L29
 Gnedin, O., Ostriker, J. 1997, ApJ, 474, 233
 Grillmair, C., Freeman, K., Irwin, M., Quinn, P. 1995, AJ, 109, 2553
 Grindlay, J., Bailyn, C., Mathieu, R., Latham, D., 1988, IAUS 126, 659
 Gunn, J. E., Griffin, R. F., 1979, AJ 84, 752
 Harris W., 1996, AJ, 112, 1487
 Johnston, K., Sigurdsson, S., Hernquist, L. 1999, MNRAS, 302, 771
 Karaali, S., 1979, AAS, 35, 241
 King, I.R., Sosin, C., Cool, A. 1995, ApJ, 452, L33
 Kroupa, P. 2001, MNRAS, in press (astro-ph/0009005)
 Leon, S., Meylan, G., Combes, F. 2000, A&A, 359, 907
 Meylan, G. 1987, A&A 184, 144
 Meylan, G. 1988, A&A 191, 215
 Meylan, G., Heggie, D. 1997, A&AR, 8, 1
 Paltrinieri, B., Ferraro, F., Paresce, F., De Marchi, G. 2001, MNRAS, in press (June 2001 issue), astro-ph/0102331
 Paresce, F., De Marchi G. 2000, ApJ, 534, 870
 Paresce, F., De Marchi G., Jedrzejewski, R. 1995, ApJ, 442, L57
 Pulone, L., De Marchi, G., Paresce, F., 1999, A&A, 342, 440
 Renzini, A. 1985, Exp. Astr., 1, 127
 Sandage, A., Smith, L. L. 1966, ApJ 144, 886
 Takahashi, K., Portegies Zwart, S., 2000, ApJ, 535, 759
 Trager, S., King, I., Djorgovski, S. 1995, AJ 109, 218
 Veronesi, C., Zaggia, S., Piotto, G. et al. 1996, in ASP Conf. Ser. 92, eds. H. Morrison & A. Sarajedini (San Francisco: ASP), 301
 Vesperini, E., Heggie, D. 1997 MNRAS 289, 898
 Webbink, F. 1985, in Dynamics of star clusters, IAU Symp. 113, (Dordrecht: Reidel), 541
 Weidemann, V. 1987, A&A, 188, 74